MICROSTRUCTURE AND MECHANICAL PROPERTIES OF SPUTTER-DEPOSITED NANOCRYSTALLINE $W_{1-y}Mo_YO_3$ THIN FILMS

GABRIEL ALBERTO LOPEZ

Master's Program in Mechanical Engineering

APPROVED:

Ramana Chintalapalle, Ph.D., Chair

Deidra Hodges, Ph.D.

Vinod Kumar, Ph.D.

Charles H. Ambler, Ph.D.
Dean of the Graduate School

Dedication

This work is dedicated to my family and to my loving wife, Claudia and our daughter Elizabeth for all their motivation and commitment to see me through the highs and lows I faced as I worked towards completing this thesis and course work for this degree.

MICROSTRUCTURE AND MECHANICAL PROPERTIES OF SPUTTER-DEPOSITED NANOCRYSTALLINE $W_{1-y}Mo_YO_3$ THIN FILMS

by

GABRIEL ALBERTO LOPEZ, B.S.

THESIS

Presented to the Faculty of the Graduate School of

The University of Texas at El Paso

in Partial Fulfillment

of the Requirements

for the Degree of

MASTER OF SCIENCE

Department of Mechanical Engineering

THE UNIVERSITY OF TEXAS AT EL PASO

December 2017

Acknowledgements

I would like to express my appreciation to my advisor Dr. Ramana Chintalapalle, for giving me the opportunity to work under his guidance and support for this research towards my Master's degree. I cannot say how thankful I am for accepting me into your research group as an undergraduate many years ago and helping me with funding and opportunities. I would have never received anywhere else. It was in your materials and manufacturing process class which sparked my interest into materials engineering, especially at the interface of materials and mechanical engineering. I would like to also thank Dr. John Jones and Dr. Neil Murphy for the exposure I received with them at the Airforce Research Laboratory in Dayton, OH. I cannot go without mentioning my groupmates past and present especially Dr. Ernesto Rubio and Dr. Gustavo Martinez. Along with Dr. Ramana, Dr. Rubio and Dr. Gustavo played an important role into integrating me into the dynamics of the research group. They each passed down their knowledge on the specifics of the equipment we use and the importance of our field. Thank you to everyone who has helped me along this path to receiving this degree.

Abstract

Currently, there is a wide-spread interest in the design and development of indium (In) free transparent conductive oxides (TCOs) for utilization in photovoltaics and optoelectronics. Tungsten oxide (WO_3)-based materials are being explored for their utilization in solar cells, photo-electrochemical cells (PECs), electrochromic (EC) "smart windows," information displays, variable reflectance mirrors, and photo-detector materials. Designing ternary compounds or composite/hybrid structures coupled with tailoring the nano-architectures of WO_3-based materials has been considered to be attractive develop potential candidates with enhanced performance. In this context, in this thesis work, an attempt is made to prepare W-Mo-O nanocomposite films, which can be considered as structural and electrode materials in photo-related energy technologies. W-Mo-O films were sputter-deposited onto Si(100) by varying the growth temperature (T_s=25-500 ^oC); Mo content was varied in the range of y=0.05–0.15 by employing the W-Mo target with a variable Mo content. Structural and mechanical characterization was performed to understand the combined effect of the Mo content and T_s on the structure and mechanical behavior of W-Mo-O films. The effect of T_s is significant on the growth and microstructure of W-Mo-O films. The effect of the Mo-content is reflected in elevating the T_s needed for film crystallization coupled with the average grain-size reduction. W-Mo-O films were amorphous for Ts≤300 ^oC, at which point amorphous-to-crystalline transformation occurs. Monoclinic (m) W-Mo-O nanocomposite films exhibit a combination of m-WO_3 and m-MoO_3 phases with m-WO_3 being predominant in the matrix. The peak intensities of the m-MoO_3 phase increases with increasing Mo-content. The nanoindentation results indicate a non-monotonic mechanical response in terms of hardness (H) and reduced elastic modulus (E_r) of the deposited films with increasing T_s. The effect of microstructure evolution is remarkable on the mechanical properties. The W-Mo-O with y=0.05 exhibit maximum H (21 GPa) and E_r (216 GPa), where Mo-incorporation induced enhancement in mechanical characteristics is pronounced. Based on the results, structure-composition-mechanical property correlation in W-Mo-O films is established.

Table of Contents

List of Tables

List of Figures

Chapter 1: Introduction

Transition-metal oxide (TMO) based insulating and/or semiconducting materials find widespread applications in many of the current advanced functional and smart device technologies. In recent years, nanostructuring has emerged as one of the best tools to unlock their full potential in current and emerging technological applications. Among the TMOs, tungsten oxide (WO_3) has been widely explored due to exceptionally versatile and unique characteristics that the material can offer in its intrinsic form or when embedded in a multi-component composite oxide structure. Currently, WO_3-based nanostructured powders, fibers, nanowires, and thin films/coatings are being explored for their application in solar cells, photo-electrochemical cells (PECs), electrochromic (EC) "smart windows," information displays, variable reflectance mirrors, chemical and electrochemical sensors, lithium batteries, photocatalysis, and photo-detector materials. However, ever increasing demand for performance and efficiency enhancement is constantly driving the thrust to further enhance the performance of WO_x-based materials, especially for application in EC devices, chemical sensors, and energy conversion and storage technologies.

Recently, WO_3 thin films and coatings are also highly researched to design transparent conducting oxide (TCO). This is primarily due to the optical, electrical, and structural characteristics of WO_3 [1-5]. WO_3 is also a member of materials known as chromogenic materials due to the coloration effects it possess from different fabrication techniques [11-14,]. Some of these applications include solar cells, photo-electrochemical cells (PECs), electrochomic (EC), variable reflectance mirrors, electrochemical sensors, photo-catalysis, and photo-detector materials [2-10]. The increase in efficiency for these applications and the demand of their design lead to develop the performance of the tungsten-oxide material systems. The focus of the present thesis work is towards the design and development of transparent electrode materials based on molybdenum (Mo) doped WO_3.

Transparent conducting oxides (TCOs) are wide band gap semiconductors (E_g>3 eV) with desired electrical conductivity (>$10^3/\Omega\cdot$cm). The TCOs are typically rendered degenerate by native or substitutional doping of electron concentrations between 10^{20}-10^{21}/cm^3. TCOs are essential components in multilayered photovoltaic devices and must be carefully processed to maximize optical transmissivity in the visible range of the electromagnetic spectrum, while achieving minimal electrical resistivity. Indium-doped tin oxide (ITO) is the most common TCO for active devices. ITO is an ideal transparent conductor. However, the scarcity of indium, which is influencing the increasing costs and preventing large-scale use of ITO in low-cost photovoltaic energy conversion [6,7]. Therefore, the scientific and research community have directed the efforts investigating the low indium-or indium free TCOs. In this context, the present work is directed towards the synthesis, characterization and mechanical property evaluation of Mo-doped WO_3 nanocomposite thin films for TCO applications. The impetus for the present work is derived from the following considerations.

Designing ternary compounds or composite/hybrid structures coupled with tailoring the nano-architectures of WO3- based materials has been considered to be attractive to develop potential candidates with enhanced performance. While a wide variety of possibilities exist to tailor the microstructure and morphology in nanostructures of WO_3 to achieve the desired properties for a given technological application, current research in metal-doped tungsten oxide based ternary compounds is very promising to meet the requirements of numerous applications in environmental, energy, and industrial engineering sectors. Doping or designing composite/ hybrid oxides using alkali ions, such as Li, K, and Na, as well as other transition metal ions, such as Ti, V, Cr, and Mn, into WO_3 has been considered in the literature for improving the photo-response or electrochemical activity. The present work was focused towards the ternary system resulting from doping of molybdenum (Mo) into tungsten oxide, which can be chemically represented by the formula $W_{1-y}Mo_yO_3$. It has been reported that addition of Mo leads to enhanced visible light photo-catalytic activity, electrochromism, photochromism, electrical conductivity, optical transparency, and high absorption band in a wide range spectrum as compared to pure WO_3.

Interestingly, the absorption band of MoO_3 is close to the maximum of the spectrum of human eye sensitivity. Therefore, it is imperative consider designing the TCOs based on W-Mo-O thin films which is the focus of the present thesis work. The following sections will provide the background information about the structure, phase stability and properties of WO_3 which will be quite useful to understand the significance of the present work and results presented and discussed.

1.1. Structure and Phase Stability of WO_3

WO_3 is a complex material to understand in the view of microstructure and thermal stability. This is due to the several crystal structures found from various processing conditions. Microstructures range from cubic, tetragonal, orthorhombic, hexagonal, triclinic, and monoclinic which is true for pure WO_3 and oxygen deficient WO_3 [24-28]. The phase transitions of WO_3 can be centered on the cubic ReO_3 structure in a distorted view [31,32]. The ever changing phases of WO_3 are largely dependent on processing temperature. It follows from low temperature from triclinic at ~30^{o}C then shifts between 30^{o}C to 330^{o}C to a monoclinic phase, then to a orthorhombic phase between 330^{o}C and 740^{o}C then above 740^{o}C a tetragonal phase is found [24-32]. From the research that has been gathered for WO_3 and doped – WO_3 composite structures, it is of high importance to understand what the incorporation of Mo within WO_3 and the affect substrate temperature (T_s) has on the microstructure. This is important in order to fine tune the properties and efficiency of the films in this study. Knowing the robustness of the mechanical and structural properties that the W-Mo-O films poses is the key to knowing their performance in practical devices such as ECs, photovoltaics and chemical sensors. A failure to know the degradation of these properties within the elements of their proposed application would lead to a short lifespan with low reliability. Furthermore, a complication and a priority in research has been the focus on incorporating WO_3 based oxides on flexible substrates with an emphasis on the nano-mechanical characteristics [12,35-38]. The research that has been performed on WO_3 has largely focused on electrical properties [44], surface and interface of WO_3 [76], optical properties [5,9], and structural and crystallinity of WO_3 [77,78]. As for W-Mo-O films, the research as mostly focused on optical

and electronic structure [12,19,20,24]. This leaves a lack in understanding mechanical properties of W-Mo-O films and the changes induced by Mo. In order to tune relevant properties for any application mentioned earlier, a mechanical dependence on structure configuration is needed. From what has been discussed, the work that is presented is focused on deriving a mechanical-structure property relationship amongst understanding what T_s and Mo effects on WO_3 intrinsic properties. The processing methods for the studied films were carried out using RF magnetron sputter deposition.

1.2 Metal Doping into WO_3

It is well known the phase stability and intrinsic properties of WO_3 are dependent on varying processing conditions and play a crucial role in the enhancement of its performance, doping WO_3 can play a beneficial role in attaining the desired properties for a specific application [15,16,17,44,76,77]. The dopants for these WO_3 systems range from alkai ions and transition metals such as Li, K, Na, and Ti, V, Cr, and Mn. These type of dopants have been found to augment the photo-response and electrochemical [3, 5, 11, 13-19]. Another transition metal that has been researched as a dopant is molybdenum (Mo). Incorporating Mo into WO_3 has been found to develop the electrical conductivity, optical transparency, photochromism, and electrochromism [19, 20, 21, 22]. The enhancement of Mo has on WO_3 has led to it gaining attention from researchers for their exploration in pump impellers, chemical sensors, and opto-electronics [12,25,26]. However the enhancement may be of any dopant, the applications and technologies that have been favorable for WO_3 and mixed WO_3 composites are all dependents on microstructure and properties. These derive from either chemical vapor depositions (CVD) or physical vapor depositions (PVD).

1.3 Significance of the Present Work

The properties and performance of WO_3 materials are highly influenced by the structure and composition. In this context, understanding the combined effect of Mo incorporation and

processing temperature (T_s) on the structure is quite important in order to tune the properties and performance of W-Mo-O films. However, while it is well known that the physical and chemical properties will depend on the dopant concentration and chemistry, the structural and mechanical durability of W-Mo-O films is imperative for their integration into practical devices, specifically in photovoltaics, PECs, and chemical sensors, with a long shelf life and excellent reliability. Furthermore, in view of their emerging applications in PECs and sensors, the mechanical characteristics of W or Mo based oxide films are quite important parameters for designing stress-free multilayered device structures on both rigid and flexible substrates. Additionally, in recent years, the importance of nanomechanical characterization of W-oxide based materials for their effective integration into chemical sensors and photovoltaics on flexible substrates has been surfacing as the priority research area. The impetus for this work is, therefore, to fill the knowledge gap by establishing a structure-mechanical property correlation in W-Mo-O films. The earlier attempts in the literature shed light on the optical modification and electronic structure changes in WO3 as a result of Mo doping. Several of the earlier reports available to date addressed the optical and electrochemical properties of thin films or nanostructured W-Mo-O. However, unfortunately, not much is known about the mechanical properties of W-Mo-O films and their relevance to the Mo content. Furthermore, a structure-composition-mechanical property correlation, which is most important in order to provide a road-map to tune the properties and phenomena for aforementioned technological applications, in Mo doped WO_3 films is totally missing at this time. Therefore, the present thesis work was focused towards the fundamental understanding of the combined structure-composition effect on the mechanical properties of Mo-incorporated nanostructured W-Mo-O films made by sputter-deposition. In addition to establishing such a structure-property relationship, as presented and discussed in this thesis, we demonstrate enhanced, superior mechanical properties of nanostructured W-Mo-O films compared to those existing in the literature to date. The results of the present work are expected to contribute to the detailed understanding of the structural and mechanical properties of W-Mo-O films, suitable for inorganics/organics-based photovoltaic devices.

Chapter 2: Literature Review

It is well known that WO_3 is a highly important and well-studied transition metal oxide (TMO). The importance of this material is due to its interesting properties that are exhibited from various processing conditions. Electronic, chromogenic, optical and structural properties are found in intrinsic WO_3 or when doped with another material. The multi material oxide system is create to enhance the properties of the doped material. Applications for WO_3 include optoelectronics, microelectronics, smart windows, selective catalyst, gas sensors and reading and writing devices [79]. As mentioned before, WO_3 and doped WO_3 systems are intensely studied for electrical, optical, chemical, and structural properties which is what the majority of literature is focused on leaving the study on mechanical properties lacking. These properties in thin films such as WO_3, TiO_2, MoO_3 and other TMOs are tailored to increase efficiency against current standards in their respective application. However focusing on Nano-mechanical characteristics can help implement these materials into current technologies or advancement by studying failure and mechanical response of varying application demands.

WO_3 thin films are generally complex to understand due to the many diverse ways of processing them. Crystal structure, electronic, morphology and other highly important properties have varying outcomes depending on the fabrication conditions and methods i.e. chemical and physical deposition methods [79]. For instance structural and thermal stability are all dependent on phase structure of WO_3 which vary from monoclinic, triclinic, tetragonal, cubic, hexagonal and orthorhombic [16-18, 44]. Vemuri et al. [44] have previously reported how substrate temperature effects crystallization of intrinsic WO_3 grown by RF magnetron sputter deposition. Their observations found by XRD reveals lower fabrication temperatures yield amorphous samples (~24^{o}C to 200^{o}C) which then a phase transformation is seen elevating substrate temperature to 300^{o}C. The XRD patterns observed from room temperature to 200^{o}C are very broad and become narrow with 300^{o}C corresponding to monoclinic WO_3 (m-WO_3) (002). When they further increased substrate temperature to 400^{o}C and 500^{o}C, patterns pertaining to tetragonal WO_3 (t-WO_3) are reported [44].

Madhavi et al. have fabricated WO_3 thin films by RF magnetron sputter deposition by varying substrate temperature between 30ºC and 400ºC, at an oxygen partial pressure of 6E-2 Pa and a deposition pressure of 4 Pa. They reported on effects of structural, morphological, optical and electrochromic properties [80]. XRD measurements revealed that the sample grown at 30ºC were amorphous in nature and explained this is a typical characteristic of sputtered deposition films grown at approximately room temperature [76, 80]. They observed upon increasing substrate temperature to 200ºC and 300ºC, the orthorhombic phase of WO_3 becomes dominant. Once they increased growth temperature to 400ºC, several diffraction peaks were observed for orthorhombic phase of WO_3 in a polycrystalline form [80]. Madhavi et al. also calculated the grain size for samples between 200ºC and 400ºC. They reported an increase in grain size with increasing temperature and proposed this was due to the enhancement of crystallization in the samples [80]. Through Raman spectroscopy, the chemical bonding of the films were studied. Madhavi et al. studied the morphology by using scanning electron microscopy (SEM) and atomic force microscopy (AFM). They found substrate temperature to play a role in grain size. Their findings showed grain size increased with higher temperatures ranging from 79nm to 140nm on average [80]. Along with SEM, Madhavi et al. gave details on surface conditions from AFM. Initially they found with lower substrate temperatures, the films contained spherical type grains which varied in size. Upon increasing the temperature, the surface structures develop into island structures. The also noted the changes in surface roughness which increases with elevation in temperature. Transmittance and optical band gap were also studied for the deposited films. In their findings, they found a reduction in transmittance from 79% to 50% with increasing substrate temperature [80]. With the transmittance data and AFM images gathered, Madhavi described the cause for such decrease in transmittance. They discuss the surface roughness is affecting the transmittance by scattering the light more than the less rough films [80]. Madhavi also note that Ramana et al. also found a similar response with films deposited by RF magnetron sputtering [81]. With transmittance data, Madhavi et al. found the optical band gap by using Tauc's relation. They found an increase to the optical band gap with increasing growth temperature. They assumed the improvement of

crystallinity of the films and the reduction in oxygen vacancies led to this behavior of the films optical band gap [80].

WO_3 thin films have also seen to be sensitive to oxygen content inside fabrication chamber during deposition. Vemuri et al. [76] gave a comprehensive report on RF sputtered WO_3 films with a fixed temperature while varying oxygen flow rates and the effect this had on the films surface and interface properties. For this investigation, the films were deposited by using a pure W target of 99.95% purity with substrate temperature and power kept constant at 400^{o}C and 100 W respectively. Vermuri et al. varied the oxygen gas ratio for each deposition in a wide range in order to observe any changes. Time for all depositions were fixed at 60 minutes. The deposition rate of the films (nm/min) was found to be sensitive to the oxygen content. Their initial measurements showed deposition rate was not sensitive till oxygen gas flow was above 0.75 which then a sharp decrease in growth rate takes place. The oxygen gas flow rate varied from 0.5 to 1.0 [79]. By using X-ray reflectivity (XRR), surface/interface roughness and thickness can be measured along with density of the WO_3 films. They found the samples to have an increase in density with increasing oxygen flow rate. Vemuri et al. also note the samples do not contain a very rough surface. XRD showed the samples contained a tetragonal crystal structure (001). The peak for tetragonal WO_3 broadens with increasing oxygen content. Grain size was also studied by using the XRD patterns which revealed a decreasing trend of grain size with higher oxygen flow rates. Vemuri et al. noted that oxygen content in the films may decrease the mobility of the adatoms. They report on an increase in the band gap values from 2.75 eV to 3.25 eV. They state this response in the films band gap values is due to excess oxygen content along with stress in the films and smaller crystallite size [79].

2.1 Motivation and Research Objectives

WO_3 is a fantastic material with potential to tailor important material properties with material incorporation into the system for varying applications. Applications that include microelectronics, optoelectronics, photo-voltaics, and gas sensors. Many of which depend on

structural, electronic and surface properties demanded by specific applications. These too vary amongst fabrication technique, processing parameters, and dopant species. Along with the highly important properties mentioned above, one that is of less studied in literature for pure and doped WO_3 is Nano-mechanical properties. The properties such as modulus and hardness for thin films can play an equal important role to provide efficient devices for a specified lifetime cycle. The incentive of this work is to derive correlation between the affects molybdenum plays on the structure, optical, surface and band gap by incorporating Mo into WO_3 thin films. Along with gaining an understanding how structural changes within the films by varying processing conditions has on the films hardness and modulus.

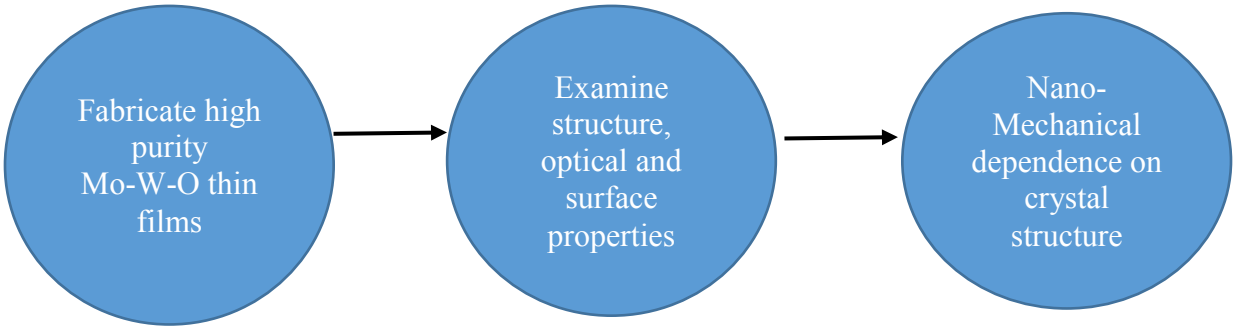

The following are the specific research objectives:

1. To fabricate W-Mo-O thin films by using reactive magnetron sputtering. Films will be prepared with various compositions by employing W/Mo alloy targets.

2. Structural analysis of the deposited W-Mo-O films to derive a comprehensive understanding of the effect of Mo and growth temperature on the resulting films.

3. Nano-mechanical and optical characterization of the W-Mo-O films to understand their mechanical behavior and optical properties.

4. Establish the structure-property relationship in W-Mo-O films.

Chapter 3: Methodology

3.1 Film Fabrication

The Mo doped WO_3 films for this study were grown by radio frequency (RF) magnetron sputtering, which is a physical vapor deposition (PVD) technique. PVD sputtering is a technique to grow thin films which is a process of when the surface of a target material is bombarded with energetic particles. When the energetic particles collide with the target material, surface atoms are then expelled and deposited on a substrate which creates coatings [thin film material technology]. In sputter deposition systems, two electrodes are placed by the substrate and target. The anode is located on the substrate side, while the cathode is placed on the target side. Both electrodes are located inside the vacuum chamber. For the sputtering process, the low pressure vacuum chamber is filled with an inert gas, typically argon (Ar). RF power is used to ionize the Ar gas which accelerate towards the target material. The ionized gas causes atoms to break from the target surface in vapor form and condense on the substrate and surrounding surfaces. The target consist of the material that will be used for the deposition of thin films [55 from Rubio thesis].

3.2 Substrates and deposition

Different substrates can be used for growing thin films depending on the study or analysis that will take place. For this study, silicon (Si) (100) and corning glass were used to deposit Mo doped WO_3 thin films. The wafers were cleaned using standard RCA cleaning procedures. The corning glass substrates were soaked in 99.9% ethanol for 20 minutes to remove any impurities from the surface. The Si wafers were cut into smaller pieces, typically 3cm x 2cm and glass samples were cut to ~2cm x 2cm. After the films were deposited, the samples grown on Si were cut into smaller pieces for different analysis. After the substrates were cleaned, they were introduced into the vacuum chamber that was used for sputtering in this study. The system is located inside the Mechanical engineering E211 lab. The system used for this study can be seen in figure 3.1.

Figure 3.1 Sputtering deposition system

Inside the deposition chamber, the substrates were placed on a sample holder that is a distance of 8cm away from the sputtering gun. The vacuum chamber was initially evacuated to a base pressure of 1.9E-5 mbar, however, each deposition was carried out at a pressure of 1.9E-2 mbar. In total, 5 targets were used for the deposition of these films. A pure tungsten (W) target was used to grown WO_3 films. A pure titanium (Ti) target was used for Ti doped WO_3 films. Three alloy targets consisting of W and molybdenum (Mo) were used for Mo doped WO_3 films. Each target varied in a mixture of weight percentage between W and Mo which varied from 95%(W):5%(Mo), 90%(W):10%(Mo) to 79%(W) and 20%(Mo). Each target consisted of the same dimensions which were 2" in diameter and 0.125" in thickness. All targets were 99.95% in purity and ordered from Plasmaterials Inc. The sputtering targets were placed on a 5.08cm sputter gun that contained a copper plate. The sputtering gun(s) were cooled down with a recirculating Polyscience water chiller. Initially, a power of 20 W was applied to the target using an Advanced Energy Cesar RF power generator while high purity Argon (Ar) was introduced to ignite the plasma. Once the plasma was ignited, the power was adjusted depending on the target(s) being

used. Before each deposition each target was pre-sputtered for 10 minutes with the shutter above the gun closed. After this step, the flow of oxygen (O_2) was incorporated into the Ar gas to create a reactive atmosphere. The flow of Ar and O_2 gas was controlled using an MKS mass flow controller. Deposition time was kept at a constant rate of 30 minutes for each sample while substrate temperature (T_s) varied. A table containing all fabrication parameters is listed below.

Table 1.1 Fabrication Parameters

Temperature	**Sample**	**Time (Hr)**	**Ar:O_2 (sccm)**
RT	W:Mo(all), WO_3, Ti-WO_3	0.5	30:10
200°C	W:Mo(all), WO_3, Ti-WO_3	0.5	30:10
300°C	W:Mo(all), WO_3, Ti-WO_3	0.5	30:10
400°C	W:Mo(all), WO_3, Ti-WO_3	0.5	30:10
500°C	W:Mo(all), WO_3, Ti-WO_3	0.5	30:10

3.3 Characterization

The characterization of these samples were done by using different techniques depending on the information that was to be gained from the sample. Structural analysis was done by using x-ray diffraction (XRD). Morphology was examined with scanning electron microscopy (SEM). Energy dispersive x-ray spectroscopy (EDS) was employed to study the elemental composition. Mechanical properties were studied with nano-indentation.

3.3.1 X-Ray Diffraction (XRD)

XRD is an analytical technique used to gain a wide variety of information for different material systems. This is done by using x-ray beams from a specific source which hits a samples surface at different incidence angles scattering the x-ray beams which are collected by a detector which provides a specific pattern pertaining to the sample's crystallographic information. In order to gain this valuable information, Bragg's law must be satisfied. The information that can be gathered relates to the crystal structure, cell dimensions and purity. In this study, grazing incidence X-ray diffraction was used to avoid any interference from the substrate and gain diffraction patterns for the films. GIXRD uses very small incidence angles to penetrate the surface of the thin films hence the use of this techniques for these sub 100nm thick films. Si substrates were used for all GIXRD studies for the W-based oxide films. The device used to analyze these intrinsic and doped WO_3 based thin films was a Bruker D8 Advanced X-ray Diffractometer (Figure 3.1). All the measurements were made ex situ as a function of growth temperature. The XRD patterns were recorded using CuKα (λ=1.54056 A) at room temperature. X-ray beams were fixed at a grazing incidence of 1^o and the detector scan mode was used with a 2θ range from 20^o to 70^o. The data was examined using EVA which is a phase evaluation software. EVA is used to check the effects of processing conditions on structural properties and lattice parameters.

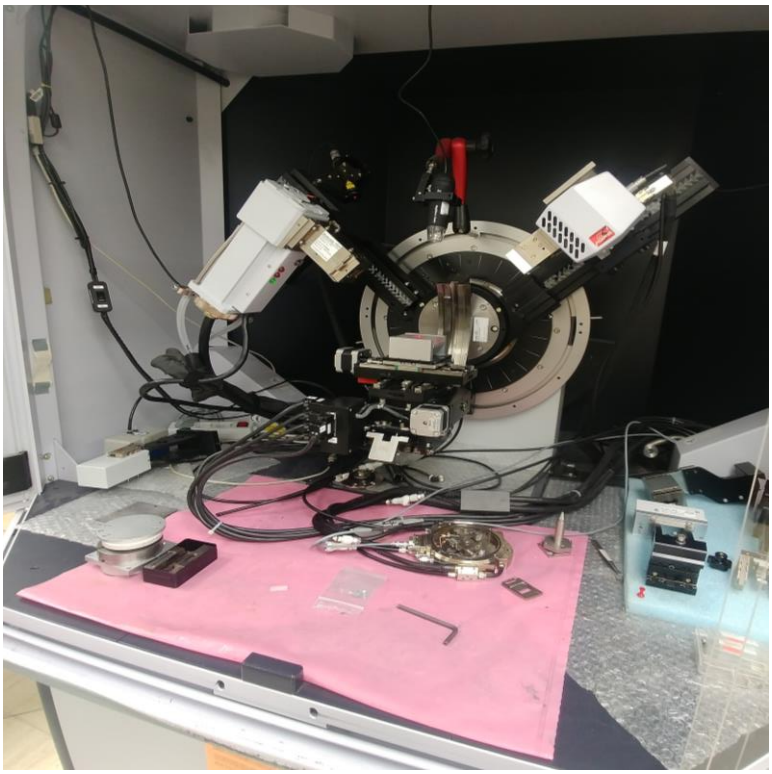

Figure 3.2 X-ray diffraction

3.3.2 SEM and EDS

For surface and morphology analysis, a Hitachi S-4790 electron microscope was used (figure 3.3). The samples were all mounted on 1 inch (diameter) stage where carbon tape was placed on top to avoid any interference from the stage during imaging. On top of the samples, a small piece of copper tape was placed to make the flow of electrons easier. The SEM provided high magnification images to help understand the evolution of grain size along and sample surface when varying the substrate temperature while processing the films. EDS analysis was done with the same setup as SEM. The machine used is an attachment to the Hitachi S-4790. EDS provides chemical characterization by using an X-ray source which interacts with the atomic structure of the sample and detected by a detector. The data that is provided are peaks which are related to the electromagnetic emission spectrum of a specific element.

Figure 3.3 SEM and EDS system

3.3.3 Nano-Indentation

Nano-mechanical characterization for all samples were investigated with the use of a Hysitron TI750 Tribo Nano-indenter. The samples were cut into small pieces and placed on a round stage. The sample surface were all probed with a triangular pyramid Berkovich diamond tip. In order to determine the maximum penetration depth that can be achieved before any interference from substrates, varying load controls were performed. The loads were performed in a large range from 50 µN to 400 µN with 50 µN steps then 600, 790, 1000 and 1050 µN were performed. Once the ideal load was found for each film set, 17 indentations were made to find hardness (H) and reduced elastic modulus (E_r) were found by taking the average of each indent. Strain sensitivity of the films were found again with their respective optimized load varying strain rates from 0.1 to 1 s^{-1}.RMS roughness for the films were found before performing indentations. Before performing any test, images of the sample surface were taken to examine if surface had no pores where loads will measured. After indentations, images were again taken to analyze load placements.

Figure 3.4 Nano-indenter

Chapter 4: Results and Discussion

The focus of this work is to gain a thorough understanding of the affects molybdenum has on the WO_3 system. Specifically on crystal structure, phase evolution, surface properties and mechanical properties. A main emphasis was to observe how change in crystal structure whether from fabrication conditions (i.e. substrate temperature) or Mo concentration had on mechanical properties of the coatings. For the various techniques needed to gain a high understanding of the fruition the films undergo, Si (100) and corning glass were used as substrates. Crystal structure, morphology, elemental composition, UV-Vis, and AFM are studied in that order. Once these are studied and information is gained, the dependence of mechanical properties on crystal structure and any changes it undertakes is examined with an effort to create a correlation between the two.

4.1. Crystal Structure

X-ray diffraction patterns of Mo doped WO_3 films are shown in Figure 4.1a-c as a function of T_s and W:Mo alloy concentration. The films grown at $T_s < 300\ ^oC$ show no appreciable peaks to WO_3 or MoO_3 which indicates the films are amorphous in nature. This was true for all sets of films fabricated regardless of Mo alloy concentration of the sputter target. A structural transformation takes place at T_s=300 ^oC. The peak observed is broad and low in intensity indicating the possible presence of small crystallites within the structural order. The minor and broad peak observed at 300 ^oC is oriented along the (020) diffraction pattern which corresponds to monoclinic WO_3 (m-WO_3) shown in Figure 4.1d. This observation indicates that a temperature of 300 ^oC is needed to activate the m-WO_3 crystal phase in the W-Mo-O films. The intensity peak (020) increases with increasing growth temperature which indicates progress towards structural stability. The monoclinic phase of WO_3 is expected as reported in literature between T_s=300 ^oC and 400 ^oC fabricated by physical vapor deposition techniques [27,43,44]. Further upon increasing T_s to the highest fabricating temperature used in this study, T_s=500 ^oC the peak of (020) m-WO_3 increases while a peak corresponding to m-MoO_3 is noted. With the presence of two peaks relating to

monoclinic WO_3 and monoclinic MoO_3, the W-Mo-O films have progressed into a two polycrystalline monoclinic matrix composite. The XRD scans for m-WO_3 with m-MoO_3 are more prominent for the sample with the highest Mo concentration of $W_{0.85}$-$Mo_{0.15}$-O_3. It should be noted, the m-WO_3 is observed with elevated temperature between 300 ^oC to 500 ^oC which has been reported to occur between 17 ^oC to 330 ^oC then undergo a phase transformation to orthorhombic WO_3 between 330 ^oC and 740 ^oC [1,27]. As mentioned before this can be attributed to deposition method and parameters where PVD techniques can yield monoclinic WO_3. Further observations into the samples grown at T_s=500 ^oC show a slight shift for the sample of $W_{0.85}$-$Mo_{0.15}$-O_3 to a higher diffraction angle. This reveals that with lower temperatures, W and Mo are intertwined and produce a film of W-Mo oxide. W and Mo atoms separate with increase of substrate temperature which leads to the WO_3 – MoO_3 composite films. Another observation was the broadening of the dominant WO_3 peak (020). Increasing the Mo content inside the films seems to be the result of this which decreases the grain size. The grain size for the films were calculated with the XRD data and the well-known and used Scherrer's equation.

$$d_{hkl} = \frac{K\lambda}{\beta cos\theta} \qquad \text{(equation 4.1)}$$

K is the shape factor which in this case was equal to 0.9 according to shape size, λ is the x-ray wavelength, β is the full width half maximum (FWHM) and θ is the angle at which it is located. By using this equation, the grain size decreased from ~ 10nm to ~6nm with Mo concentration of y = 0.05 to 0.15.

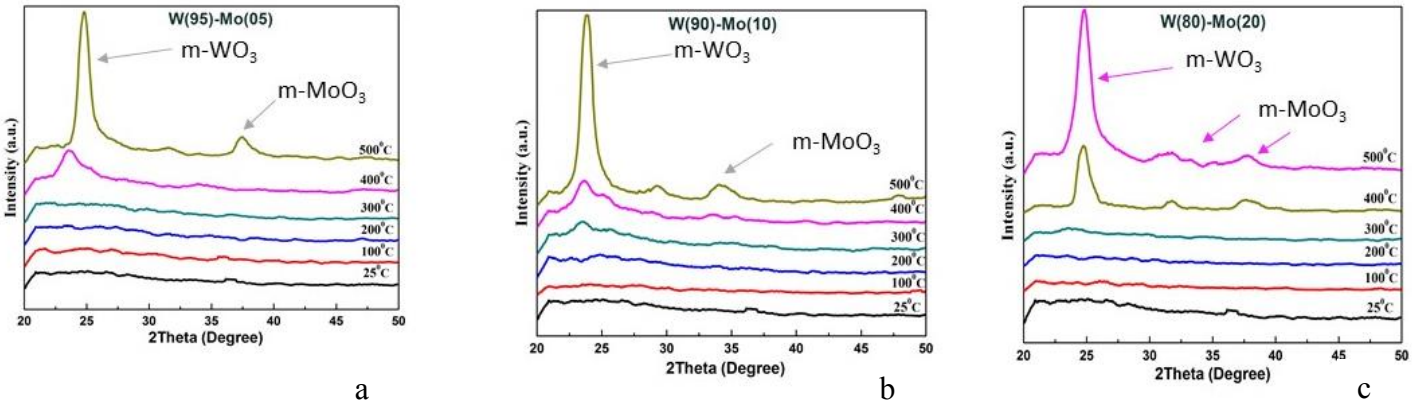

a b c

Figure 4.1 XRD patterns for all deposited samples

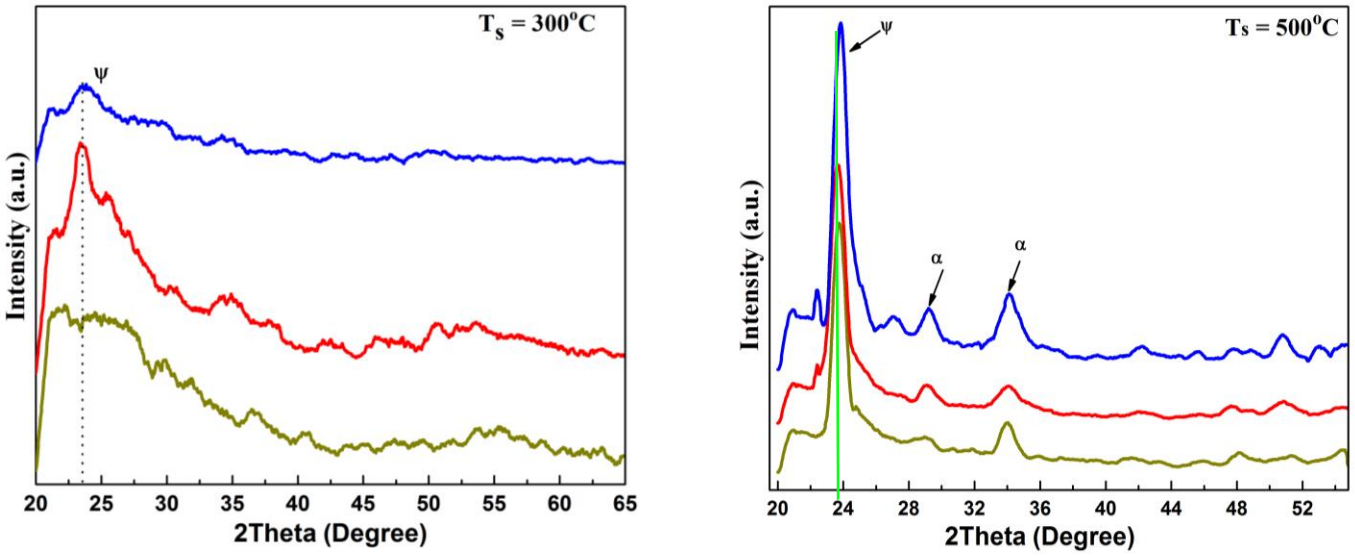

Figure 4.2 High resolution XRD scans of all samples

4.2. Surface Morphology

Scanning electron microscopy (SEM) and atomic force microscopy (AFM) were employed to understand the surface morphology evolution of the fabricated W-Mo-O thin films as a function of T_s and Mo content. The SEM and AFM images are presented in Figures 4.3a, 4.3b and 4.3c. It is clear that substrate temperature plays a vital role in the surface morphology of the films and undergoes slight differences with Mo concentration. It is seen that with all films grown at room temperature (T_s~25 ^oC) are amorphous in nature and do not contain any grains. This is true for Mo content from y = 0.05 to 0.15. 25^oC and 100^oC were left out of further morphology studies by SEM and AFM since it is well known that WO_3 based thin films exhibit amorphous features at low temperatures grown by PVD. Only those fabricated for $W_{0.95}Mo_{0.05}O_3$ films will have 25^oC and 100^oC samples shown for this study. AFM studies were carried out and confirm the presence of amorphous films at low fabrication temperatures and show the transformation at 300^oC which leads to full polycrystalline films for 400^oC and 500^oC.

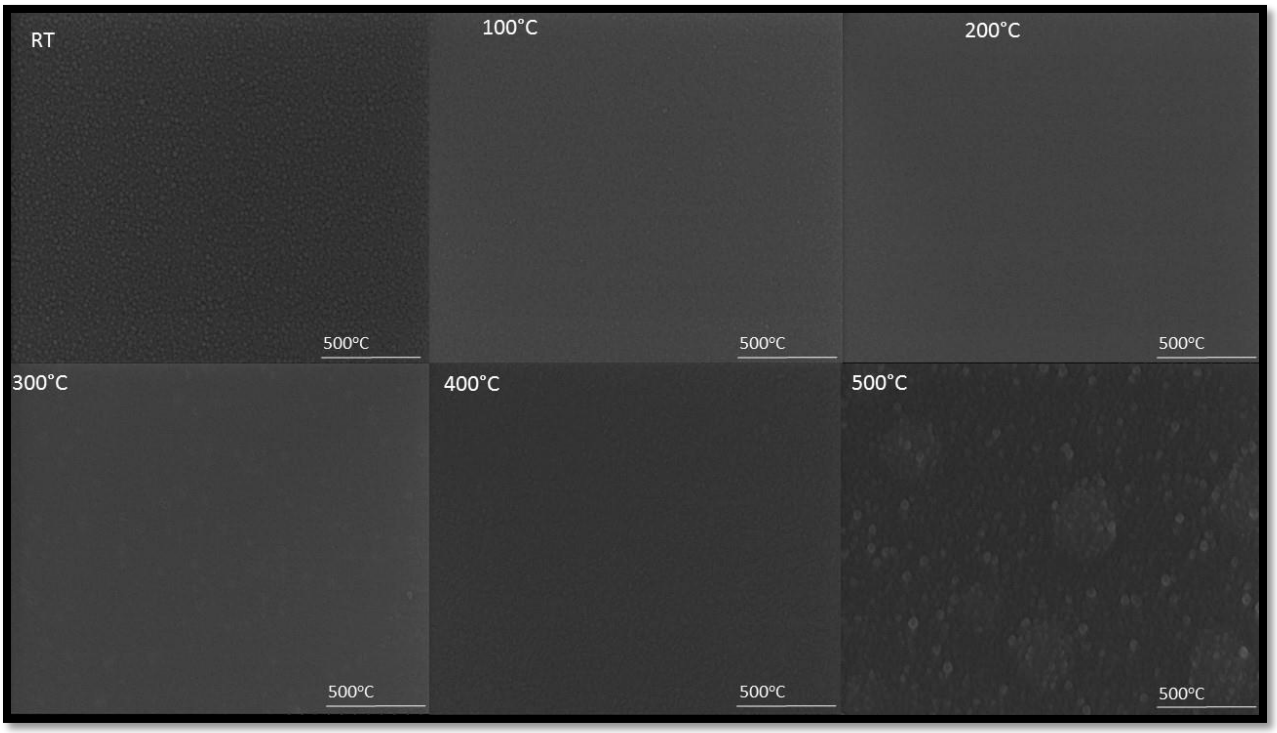

Figure 4.3a SEM for $W_{0.95}Mo_{0.05}O_3$

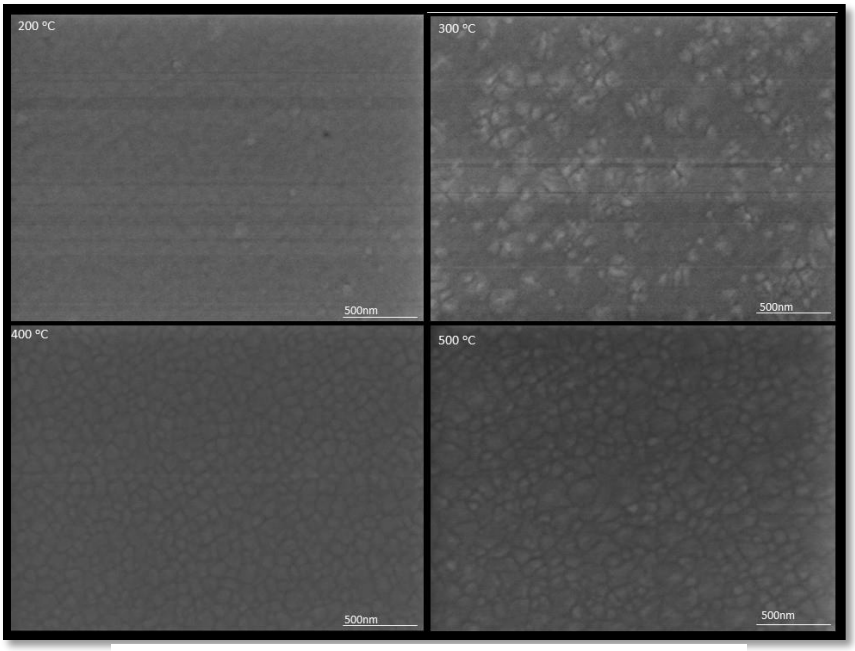

Figure 4.3b SEM for $W_{0.90}Mo_{0.10}O_3$

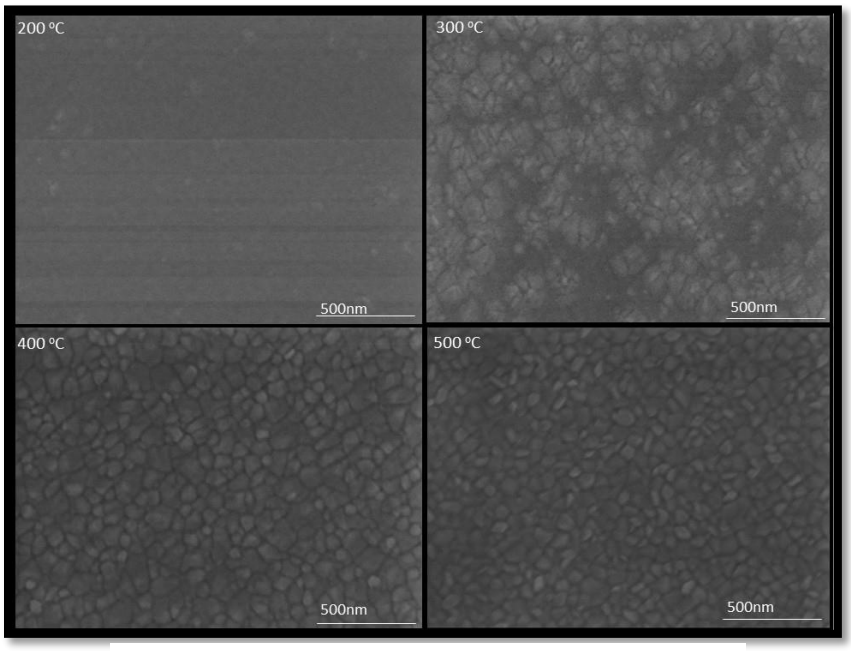

Figure 4.3c SEM for $W_{0.85}Mo_{0.15}O_3$

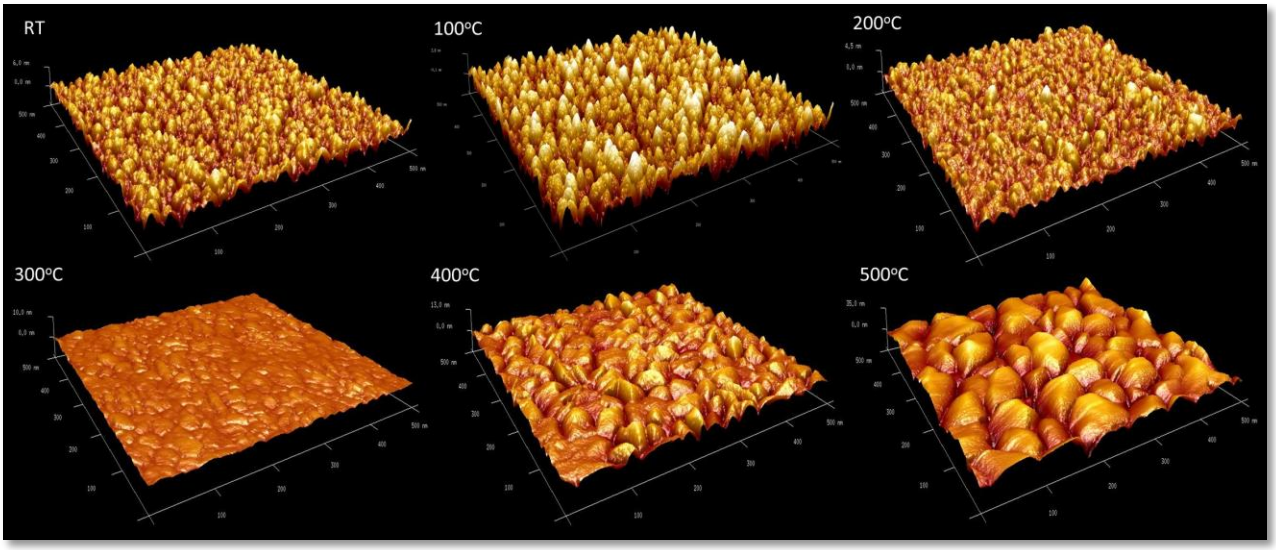

Figure 4.4a AFM 3D images for $W_{0.95}Mo_{0.05}O_3$

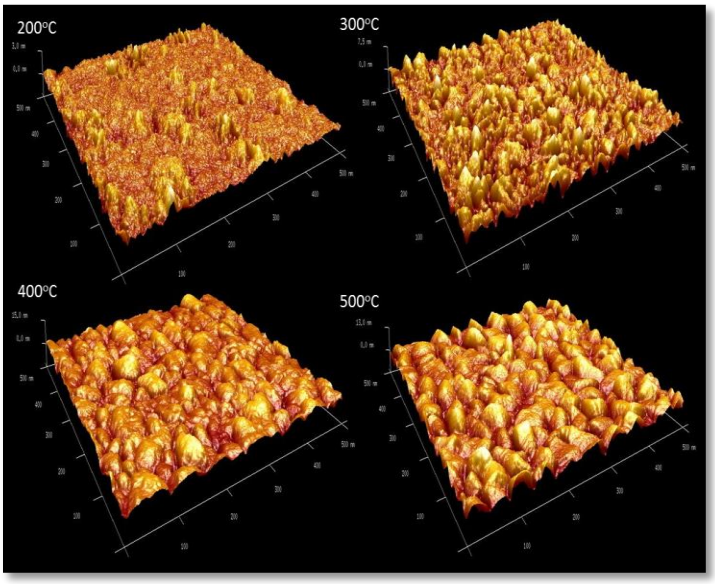

Figure 4.4b AFM 3D images for $W_{0.90}Mo_{0.10}O_3$

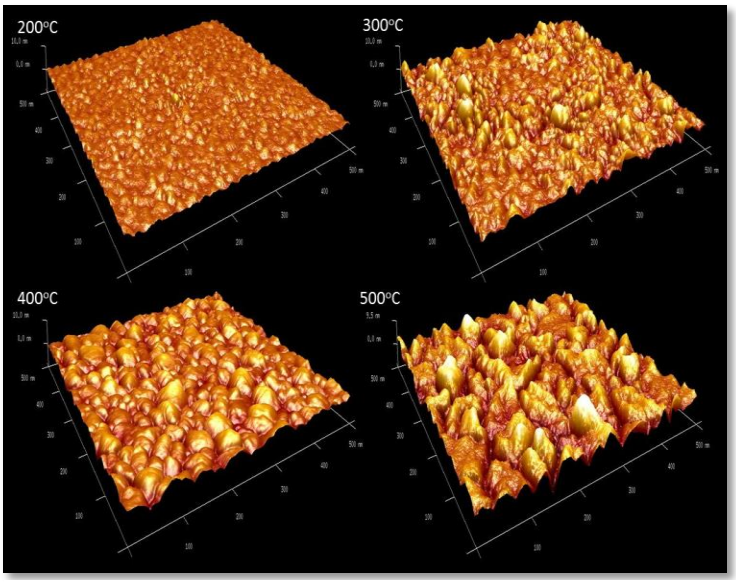

Figure 4.4c AFM 3D images for $W_{0.85}Mo_{0.15}O_3$

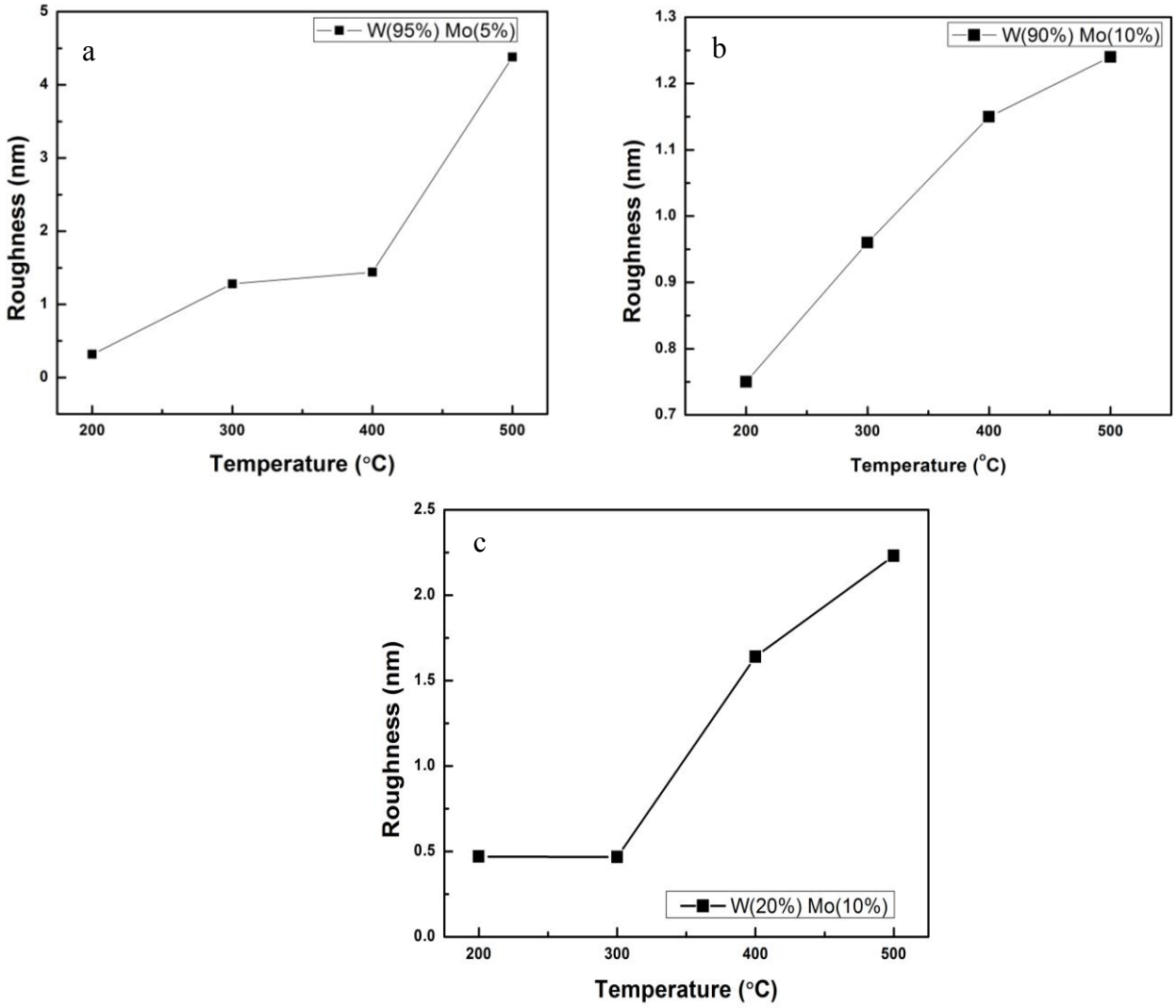

Figure 4.5 Surface roughness for all deposited samples

4.3. Optical Transmission

Apart from studying microstructure and surface features of the films, optical properties where studied to gain some insight into the optical characteristics of the films. The transmission spectra shows the $W_{y-1}Mo_yO_3$ films are transparent (Figure 4.6a-c). The amorphous films (25ºC-200ºC) provide the highest transparency for all sets across the transmission spectra. For the polycrystalline films containing WO_3 and MoO_3 the transparency decreases slightly but still remains around 70% to 79%. The film that shows the highest drop come from $W_{85}Mo_{15}O_3$ at 500ºC. The transparency drops to below 70% for the range of 50% to 790%. This can be due to Mo content within the films which causes two monoclinc polycrystalline structures to form.

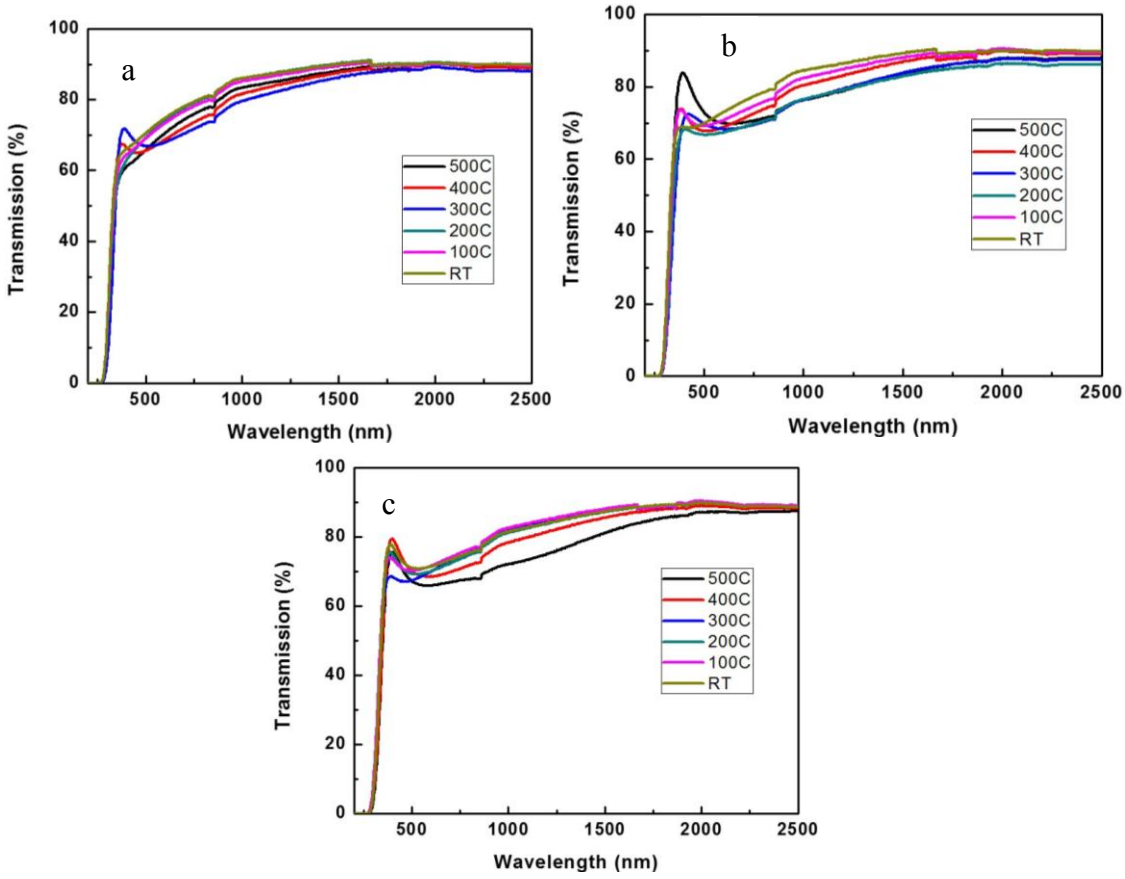

Figure 4.6 Transmission spectrum for deposited samples

4.4. Chemical Composition

Energy dispersive spectroscopy (EDS) was used to gain insight on elemental composition of the films. The measurements were carried out across the W-Mo-O film surface and an average for at% was taken. It should be noted that the oxygen content of the films was balanced at the 100 atomic percent scale. The elemental compositions between W and Mo for S1, S2 and S3 is seen in figure 4.7a, b, and c respectively. The first observation is that the total at% between W and Mo remain largely the same at ~15 at% for all films. For this trend, it can be assumed that Mo atoms are going into the W-Mo-O films as substitutional atoms for W atoms. A few points can be taken from this and steers the results to this expectation. The first is that the ionic size of W^{6+} and Mo^{6+} are very similar, 0.60A and 0.59A respectively. The second is the small difference between lattice parameter. Third the content of Mo is low within the films. The last point is that interstitial substitution involves adatoms to be similar in size for tetragonal or octahedral, 0.2 and 0.4 atomic radii [21,41-44]. Weight percentage of the films were also taken using EDS to compare to the wt% of the alloy sputtering target. The wt% of the films were found to be on par with that of the sputtering target that was used for the respective set. There was one observation regarding the films wt% ratio between Mo and W. They were lower than the targets used for sputtering which can be attributed to sputtering yield or the oxygen content on the surface of the W-Mo targets [41].

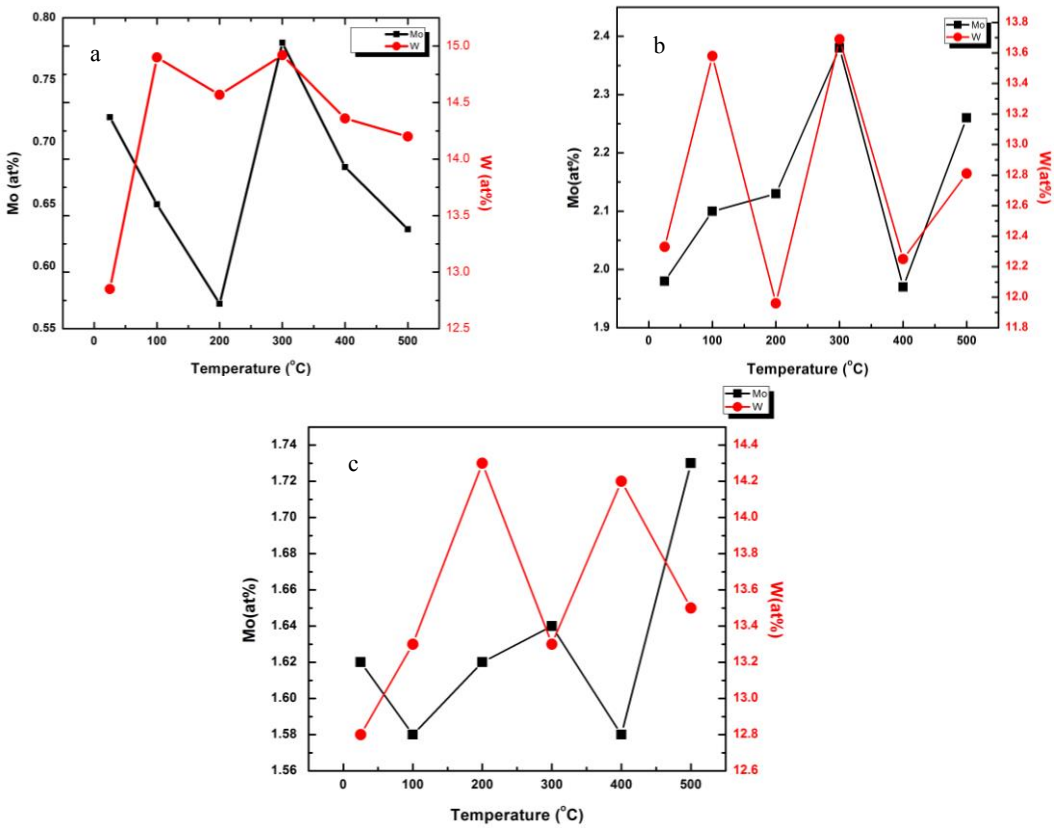

Figure 4.7 at% of deposited samples

4.5 Mechanical Properties

Nano-indentation was used to probe the samples to study their response to varying loads and effects of morphology along with Mo content. All samples were loaded first in a wide range between 50uN to 1500uN. This was done to minimize any affects the Si substrate had on the readings. A load of 300uN was found to be ideal to study the hardness and elastic modulus of the films. The hardness and modulus as a function of T_s can be seen in figure 4.8a through 4.8c. H and E for all films have a clear trend in which they don't continuously decrease or increase along the substrate temperature. Both however, share the same response to T_s for all films. Hardness increases from between ~15GPa and 17GPa to a maximum value between 18GPa and 20GPa then decreases ranging from 13GPa to ~10GPa. Elastic modulus sees a similar trend with a high value of 220GPa to a low value of 150GPa for $W_{0.85}Mo_{0.15}O_3$. Hardness and modulus stacked together for all sets can be seen in figure 4.9a and 4.9b. What is interesting in the graphs for H and E is the substrate temperature 300°C and the values for this. Hardness reaches its maximum value and modulus all share a very close value of 210 GPa. The response of the films shows that amorphous

films yield higher values of hardness and the polycrystalline films produce lower values. This can be due to defects caused by the Mo inclusion in the WO_3 films. Since T_s=300°C has a very curious phenomenon, it was used to carry out indentation depth analysis of the films. This study appears in figure 4.10 a and c. The curve for H shows a plateau that is not seen in the E curve which tells that the hardness has a higher sensitivity to the Si substrate used for fabrication. This plateau also shows H values as nearly constant which characterizes the true intrinsic hardness of the film sets. The H value shows no such drift such as H and continuously decreases then approaches the modulus of the Si substrate at ~150 GPa. The hardness and modulus of intrinsic and doped WO_3 are compared in figure 11a. Mo doped WO_3 show to have higher values in hardness and modulus as compared to intrinic WO_3. H/E_r is compared which represents an indirect way to determine the wear resistance for coatings [49-51]. When compared, films with 5 at% of Mo are ideal to produce for practical devices. This is due to an ideal value that is higher than >0.1. None of the fabricated films are greater than this value but closely resemble. Another paramter compared is H^3/E^2_r which gives an indication to the films resistance to plastic deformation [53]. Again films with lowest Mo content are ideal for this value. Figure 4.11b shows the pile-up length. The higher the value for the pile-up, the lower the films ability to recovery elastcally.

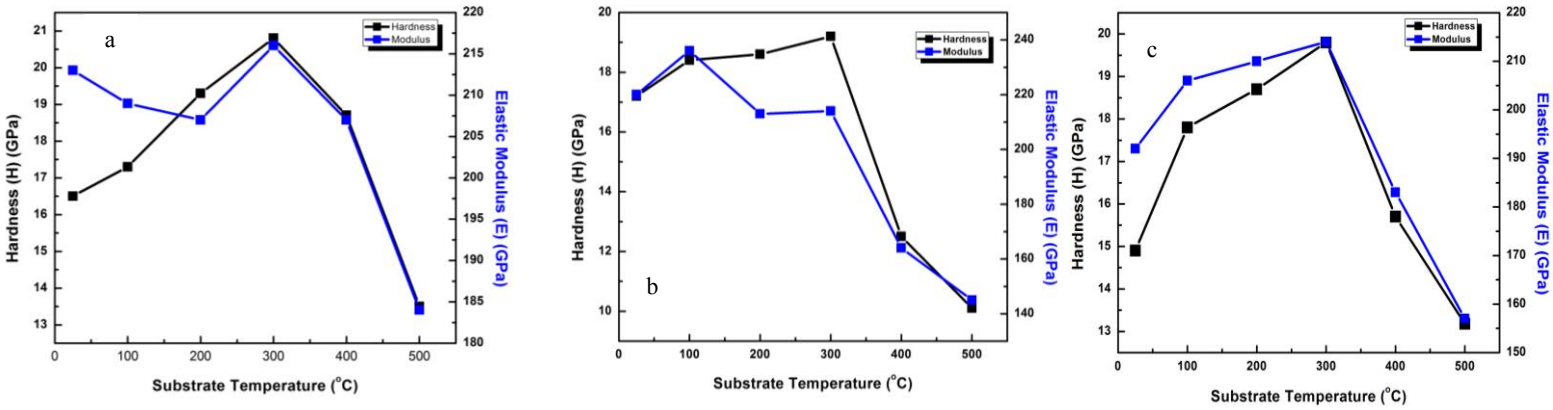

Figure 4.8 H and E as a function of T_s

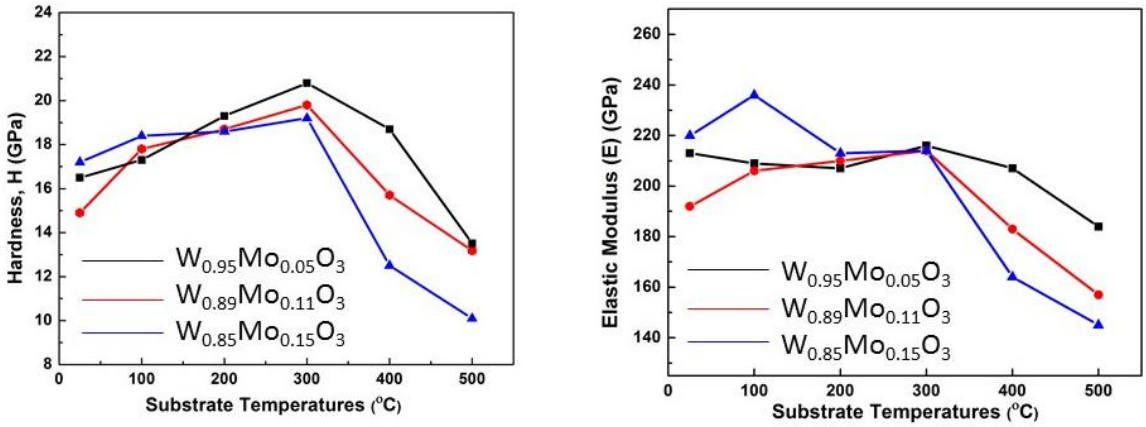

Figure 4.9 H and E for all deposited samples

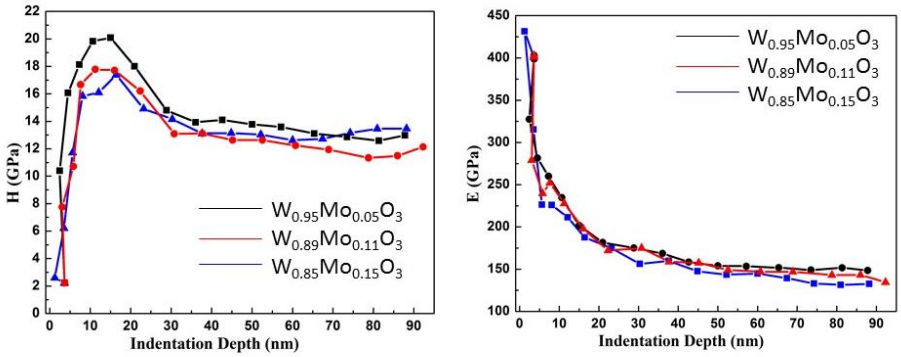

Figure 4.10 H and E as a function of indentation depth for T_s = 300°C

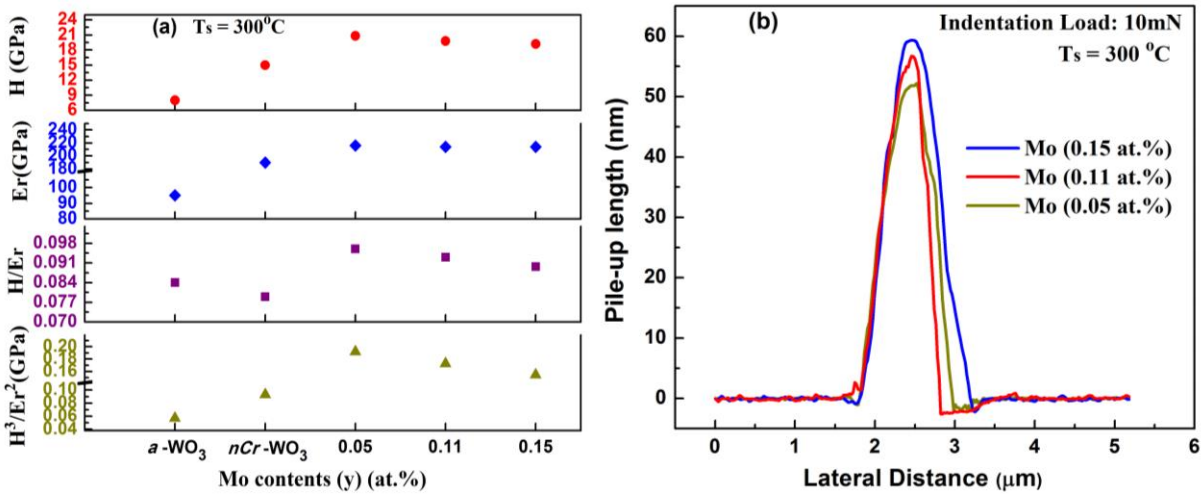

Figure 4.11 a) H, E, H/E, and H_2/H_r^2 comparison to intrinsic WO_3 b) Pile-up legnth

Chapter 5: Conclusions

Polycrystalline $W_{1-y}Mo_yO_3$ thin films were fabricated by RF magnetron sputter deposition. Fabrication parameters included varying Mo content between y = 0.05 – 0.15 and varying deposition temperature (T_s). The films were grown on Si (100) and corning glass substrates. A metal target of W-Mo varied by weight percentage (wt%) was used from W(95):Mo(5), W(90):Mo(10), and W(79):Mo(20). Microstructure and mechanical properties were strongly investigated in order to provide a detailed understanding of mechanical behavior T_s and Mo content has on WO_3. Microstructure analysis were investigated by GIXRD which indicates amorphous films from ~25ºC to 200ºC than a transition to monoclinic WO_3 between 300ºC. Fully crystalline films were formed for 400ºC and 500ºC. For samples with higher Mo content (y=0.15), a composite film was formed with two monoclinic structures, for WO_3 and MoO_3. The details gather from GIXRD were confirmed with SEM and AFM which confirms the presence of amorphous films and polycrystalline films with varying T_s. The films atomic percentage was gathered by EDS, which revealed a trend of Mo going as a substitution for W inside the matrix. It also showed the films wt% was similar to that of the alloy target used but had a decrease with the wt%. This can be assumed to sputtering yield rates or an oxidized layer forming on the target. Nano-indentation studies show a remarkable effect T_s has on mechanical properties as well as Mo content. A low Mo content of y = 0.05 showed to produce the films with the highest hardness (H) and modulus (E) with values of ~21 GPa and 216 GPa respectively. Substrate temperature showed 300ºC to be interesting as compared to amorphous and crystalline films. By varying indentation depth, hardness was shown to be strongly influenced by the Si substrate. From the studies performed it was found that having a film with the lowest Mo percentage $W_{0.95}Mo_{0.05}O_3$ produced films that best suite integration into real-world devices.

References

1. H. Zheng, J. Z. Ou, M. S. Strano, R. B. Kaner, A. Mitchell, and K. Kalantar-Zadeh; "Nanostructured Tungsten Oxide – Properties, Synthesis, and Applications" *Advanced Functional Materials*, **2011**, 21 (12), 2175-2196.

2. L. D'Arsi_e, S. Esconjauregui, R. Weatherup, Y. Guo, S. Bhardwaj, A.Centeno, A. Zurutuza, C. Cepek, and J. Robertson; "Stability of Graphene Doping with MoO_3 and I_2" *Applied Physics Letter*, **2014**, 105, 103103.

3. K.R. Reyes-Gil, Z.D. Stephens, V. Stavila, and D.B. Robinson; "Composite WO_3/TiO_2 Nanostructures for High Electrochromic Activity" *ACS Applied Materials and Interfaces*, **2015**, 7 (4), 2202-2213.

4. M. B. Johansson, P. T. Kristiansen, L. Duda, G. A. Niklasson, and L. Osterlund; " J. Phys.: Condens. Matter 28, 475792 (2016).

5. C. V. Ramana, G. Baghmar, E. J. Rubio, and M. J. Hernandez; "Optical Constants of Amorphous, Transparent Titanium-Doped Tungsten Oxide Thin Films" *ACS Applied Materials and Interfaces*, **2013**, 5 (11), 4659-4666.

6. M. B. Johansson, B. Zietz, G. A. Niklasson, and L. €Osterlund; "Optical Properties of Nanocrystalline WO_3 and WO_{3-x} Thin Films Prepared by DC Magnetron Sputtering" *Journal of Applied Physics*, **2014**, 115, 213510

7. H. Zheng, Y. Tachibana, and K. Kalantar-Zadeh, Langmuir; "Dye-Sensitized Solar Cells Based on WO_3" *Langmuir*, **2010**, 26 (24), 19148-19152.

8. B. Liu, D. Tang, Y. Zhou, Y. Yin, Y. Peng, W. Zhou, Z. Qin, and Y. Zhang; "Electrical Characterizaion of H_2 Adsorption on Hexagonal WO_3 Nanowire at Room Temperature" *Journal of Applied Physics*, **2014**, 116, 164310.

9. M. Vargas, E. J. Rubio, A. Gutierrez, and C. V. Ramana; "Spectroscopic Ellipsometry Determination of the Optical Constants of Titianium-Doped WO_3 Films Made by Co-Sputter Deposition" *Journal of Applied Physics,* **2014**, 115, 133511.

10. S. K. Deb, Sol; "Opportunities and Challenge in Science and Technology of WO_3 for Electrochromic and Related Applications" *Solar Energy Materials and Solar Cells*, **2008,** 92 (2), 245-258.

11. Z. He, Q. Liu, H. Hou, F. Gao, B. Tang, and W. Yang, ACS Appl. Mater. Interfaces 7, 10877 (2015).

12. X. Li, H. Teng, L. Zhang, J. Zhou, and M. Liu, RSC Adv. 5, 95394 (2015).
13. Y. Wu, D. Chu, P. Yang, Y. Du, and C. Lu; "Terneray Mesoporous WO_3/Mn_3O_4/N-Doped Graphene Nanocomposite for Enhanced Photocatalysis Under Visible Light Irradiation" *Catalysis Science & Technology*, **2015**, 5, 3375
14. W. Smith and Y. Zhao; "Enhanced Photocatalytic Activity by Aligned WO_3/TiO_2 Two-Layer Nanorod Arrays" *Journal of Physical Chemistry,* **2008**, 112 (49), 19635-19641.
15. W. Smith, A. Wolcott, R. C. Fitzmorris, J. Z. Zhang, and Y. Zhao, J. Mater. Chem. 21, 10782 (2011).
16. G.-F. Cai, X.-L. Wang, D. Zhou, J.-H. Zhang, Q.-Q. Xiong, C.-D. Gu, and J.-P. Tu, RSC Adv. 3, 6896 (2013).
17. M. A. Arvizu, C. A. Triana, B. I. Stefanov, C. G. Granqvist, and G. A. Niklasson; "Electrochromism in Sputter-Deposited W-Ti Oxide Films: Durability Enhancement Due to Ti" *Solar Energy Material and Solar Cells*, **2014**, 125, 184-189.
18. F. Wang, C. D. Valentin, and G. Pacchioni; "Doping of WO_3 for Photocatalytic Water Splitting: Hints from Density Functional Theory" *Journal of Physical Chemistry*, **2012**, 116(16), 8901-8909.
19. T. He and J. Yao; "Photochromism in Composite and Hybrid Materials Based on Transition-Metal Oxides and Polyocometalates" *Progress in Materials Science*, **2006**, 51(6), 810-879.
20. J. M. O-R. D. Leon, D. R. Acosta, U. Pal, and L. Castaneda; "Improving Electrochromic Behavior of Spray Pyrolised WO_3 Thin Films by Mo Doping" *Electrochimica Acta*, 2011, 56 (5), 2599-2605.
21. V. Madhavi, P. J. Kumar, P. Kondaiah, O. M. Hussain, and S. Uthanna; "Effect of Molybdenum Doping on the Electrochromic Properties of Tungsten Oxide Thin Films by RF Magnetron Sputtering" *Ionics*, **2014**, 20 (12), 1737-1745.
22. B. W. Faughnan and R. S. Crandall; "Optical Properties of Mixed-Oxide WO_3/MoO_3 Electrochromic Films" *Applied Physics Letters,* **1977**, 31, 834.

23. C. G. Granqvist, Handbook of Inorganic Electrochromic Materials (Elsevier, New York, 1995).
24. P. R. Patila and P. S. Patil; "Preparation of Mixed Oxide MoO_3-WO_3 Thin Films by Spray Pyrolsis Technique and Their Characterization" *Thin Solid Films*, **2001**, 382 (1-2), 13-22.
25. W. H. Cubberly and R. Bakerjian, Tool and Manufacturing Engineers Handbook, Desk ed. (Society of Manufacturing Engineers, Dearborn, Michigan, 1989).
26. Zheng-Hua Tan, Xue-Bing Yin, and Xin Guo; "One-Dimensional Memristive Device Based on MoO_3 Nanobelt" *Applied Physics Letters*, **2015**, 106, 023503.
27. C. V. Ramana, S. Utsunomiya, R. C. Ewing, C. M. Julien, and U. Becker; "Structural Stability and Phase Transitions in WO_3 Thin Films" *Journal of Physical Chemistry*, **2006**, 110 (21), 10430-10435.
28. L. E. Depero, S. Groppelli, I. Natali-Sora, L. Sangaletti, G. Sberveglieri, and E. Tondello, J. Solid State Chem. 121, 378 (1996).
29. E. K. H. Salje, S. Rehmann, F. Pobell, D. Morris, K. S. Knight, T. Hermannsdorfer, and M. T. Dove; "Crystal Structure and Paramagnetic Behavior of ε – WO_{3-x}" *Journal of Physics: Condensed Matter*, **1997**, 9 (31), 6563.
30. M. Boulova and G. Lucazeau; "Crystallite Nanosize Effect on the Structural Transitions of WO_3 Studied by Raman Spectroscopy" *Journal of Solid State Chemistry*, **2002**, 167 (2), 425-434.
31. B. Johansson, G. Baldissera, I. Valyukh, C. Persson, H. Arwin, G. A. Niklasson, and L. Osterlund; "Electronic and Optical Properties of Nanocrystalline WO_3 Thin Films Studied by Optical Spectroscopy and Density Functional Calculations" *Journal of Physics: Condensed Matter*, **2013**, 25 (20), 205502.
32. I. M. Szilagyi, B. Forizs, O. Rosseler, A. Szegedi, P. Nemeth, P. Kiraly, G. Tarkanyi, B. Vajna, K. Varga-Josepovits, K. Laszlo, A. L. Toth, P. Baranyai, and M. Leskela; "WO_3 Photocatalysts: Influence of Structure and Composition" *Journal of Catalysis*, **2012**, 294, 119-127.

33. Tungsten: Properties, Chemistry, Technology of the Element, Alloys, and Chemical Compounds, edited by E. Lassner and W.-D. Schubert (Kluwer Academic, 1999).
34. Y. Du, M. Gu, T. Varga, C. Wang, M. E. Bowden, and S. A. Chambers; "Strain Accommodaiton by Facile WO_6 Octahedral Distortion and Tilting During WO_3 Heteroeptiaxy on $SrTiO_3$ (001)" *ACS Applied Materials and Interfaces*, **2014**, 6(16), 14253-14258.
35. K. Zeng, F. Zhu, J. Hu, L. Shen, K. Zhang, and H. Gong; "Investigation of Mechanical Properties of Transparent Conducting Oxide Thin Films" *Thin Solid Films,* **2003**,443(1), 60-65.
36. J. L. Enriquez-Carrejo, M. A. Ramos, J. Mireles-Jr-Garcia, and A. Hurtado-Macias; "Nano-Mechanical and Structural Study of WO_3 Thin Films" *Thin Solid Films,* **2016**, 606,148-154.
37. S. Hu, N. S. Lewis, J. W. Ager, J. Yang, J. R. McKone, and N. C. Strandwitz; "Thin Films Materials for the Protection of Semiconducting Photoelectrodes in Solar fuel Generators" *Journal of Physical Chemistry*, **2005**, 119 (43), 24201-24228.
38. O. R. Nunez, A. J. Moreno Tarango, N. R. Murphy, and C. V. Ramana; "Nitrogen Incorporation and Composition Facilitated Tailoring of the Optical Constants and Dispersion Energy Parameters of Tungsten Oxynitride Films" *Journal of Alloys and Compounds*, **2016**, 683, 292-301.
39. W. C. Oliver and G. M. Pharr; "An Improved Technique for Determining Hardness and Elastic Modulus Using Load and Displacement Sensing Indentation Experiments" *Journal of Materials Research*, **1992**, 7 (6), 1564-1583.
40. H. Nili, K. Kalantar-zadeh, M. Bhaskaran, and S. Sriram; "In Situe Nanoindentation: Probing Nanoscale Multifunctionality" *Progress in Materials Science*, **2013**, 58 (1), 1-29.
41. D. Guttler, B. Abendroth, R. Grotzschel, and W. Moller; "Mechanisms of Target Poisoning During Magnetron Sputtering as Investigated by Real-Time in Situ Analysis and Collisional Computer Simulation" *Applied Physics Letters,* **2004**, 85, 6134.

42. M. Vargas, D. M. Lopez, N. R. Murphy, J. T. Grant, and C. V. Ramana; "Effect of W-Ti Target Composition on the Surface Chemistry and Electronic Structure of WO_3-TiO_2 Films Made by Reactive Sputtering" *Applied Surface Science*, **2015**, 353, 728-734.
43. N. R. Kalidindi, F. S. Manciu, and C. V. Ramana; "Crystal Structure, Phase, and Electrical Conductivity of Nanocrystalline $W_{0.95}Ti_{0.05}O_3$ Thin Films" *Applied Materials Interfaces*, **2011**, 3 (3), 863-868.
44. R. S. Vemuri, B. K. Kamala, S. K. Gullapalli, and C. V. Ramana; "Effect of Structure and Size on the Electrical Properties of Nanocrystalline WO_3 Films" *Applied Materials Interfaces*, **2010,** 2(9) 2623-2628.
45. N. M. G. Parreira, N. J. M. Carvalho, and A. Cavaleiro; "Synthesis, Structural and Mechanical Characterization of Sputtered Tungsten Oxide Coatings" *Thin Solid Films,* **2006**, 510 (1), 191-196.
46. W. D. Nix and H. J. Gao; "Indentation Size Effects in Crystalline Materials: A Law for Strain Gradient Plasticity" *Journal of the Mechanics and Physics of Solids*, **1998**, 46(3), 411-425.
47. R. Saha and W. D. Nix; "Effet of the Substrate on the Determination of Thin Film Mechanical Properties by Nanoindentation" *Acta Materialia*, **2002**, 50 (1), 23-38.
48. D. Beegan, S. Chowdhury, and M. T. Laugie; "The Nanoiondentation Behaviour of Hard and Soft Films on Silicon Substrates" *Thin Solid Films*, **2004**, 466(1), 167-174.
49. A. Leyland and A. Matthews; "On the Significance of the H/E Ratio in Wear Control: A Nanocomposite Coating Approach to Optimised Tribological Behaviour" *Wear*, **2000**, 246(1), 1-11.
50. E. Santos, Jr., K. D. P. Nascimento, and S. S. Camargo, Jr., J. Mater. Res. 16, 1148 (2013).
51. C. A. Charitidis; "Nanomechanical and Nanotribological Properties of Carbon-Based Thin Films: A Review" *International Journal of Refractory Metals and Hard Materials*, **2010**, 28(1), 51-70.

52. J. Musil, F. Kunc, H. Zeman, and H. Polakova; "Relationships Between Hardness, Young's Modulus and Elastic Recovery in Hard Nanocomposite Coating" *Surface and Coatings Technology*, **2002**, 154 (2), 304-313.
53. J. M. Harrison, D. Goldbaum, T. C. Corkery, C. J. Barrett, and R. R. Chromik; "Nanoindentaion Studies to Separate Thermal and Optical Effects in Photo-Softening of Azo Polymers" *Journal of Materials Chemistry C,* **2015**, 3, 995-1003.
54. M. Mayo and W. Nix; "A Micro-Indentation Study of Superplasticity in Pb, Sn, and Sn-38 wt% Pb" *Acta Metallurgica,* **1988**, 36(8), 2183-2192.
55. R. C. Picu; "A Mechanism for the Negative Strain-Rate Sensitivity of Dilute Solid Solutions" *Acta Materialia,* 52 (12), 3447-3458.
56. S. Kumar; "Inverse Behavior of the Onset Strain of Serrated Flow"*Scripta Metallurgica et Materialia,* **1995**, 33 (1), 81-86.
57. M. Abbadi, P. Hahner, and A. Zeghloul; "On the Characterization of Portevin-Le Chatelier Bands in Aluminum Alloy 5182 Under Stress-Controlled and Strain-Controlled Tensile Testing" *Materials Science and Engineering:A,* **2002**, 337 (1), 194-201.
58. A. Nortmann and Ch. Schwink; "Characteristics of Dynamic Strain Ageing in Binary f.c.c Copper Alloys-II. Comparison and Analysis of Experiments on CuAl and CuMn" *Acta Materialia,* **1997**, 45 (5), 2051-2058.
59. R. D. Shannon; "Revised Effective Ionic Radii and Systematic Studies of Interatomic Distances in Halides and Chalcogenides" *Acta Crystallographica Section A,* **1976**, 32, 751-767.
60. S. S. Kumar, E. J. Rubio, M. Noor-A-Alam, G. Martinez, S. Manandhar, V. Shutthanandan, S. Thevuthasan, and C. V. Ramana; "Structure, Morphology, and Optical Properties of Amorphous and Nanocrystalline Gallium Oxide Thin Films" *Journal of Physical Chemistry C*, **2013**, 117 (8), 4194-4200.

61. C. V. Ramana, K. Kamala Bharathi, A. Garcia, and A. L. Campbell; "Growth Behaviour, Lattice Expansion, Strain and Surface Morphology of Nanocrystalline, Monoclinic HfO_2 Thin Films" *Journal of Physical Chemistry C*, **2012**, 116(18), 9955-9960.
62. C. V. Ramana, M. Noor-A-Alam, J. J. Gengler, and J. G. Jones; "Growth, Structure, and Thermal Conductivity of Yttria-Stabilized Hafnia Thin Films" *ACS Applied Materials and Interfaces,* **2012,** 4(1), 200-204.
63. K. A. Gesheva, T. Ivanova, B. Marsen, B. Cole, E. L. Miller, and F. Hamelmann, Surf. Coat. Technol. 201, 9377 (2007).
64. K. A. Gesheva and T. Ivanova; " A Low-Temperature Atmospheric Pressure CVD Process for Growing Thin Films of MoO_3 and MoO_3-WO_3 for Electrochromic Device Applications" *Chemical Vapor Deposition*, **2006**, 12 (4), 231-238.
65. A. Vomiero, G. D. Mea, M. Ferroni, G. Martinelli, G. Roncarati, V. Guidi, E. Comini, and G. Sberveglieri; "Preperation and Microstructural Characterizaiton of Nanosized Mo-TiO_2 and Mo-W-O Thin Films by Sputtering: Tailoring of Composition and Porosity by Thermal Treatment" *Materials Science and Engineering: B*, **2003**, 101(1), 216-221.
66. W. E. Farneth, E. M. McCarron, A. W. Sleight, and R. H. Staley; "Comparison of the Surface Chemistry of Two Polymorphic Forms of Molybdenum Trioxide" *Langmuir,* **1987**, 3, 217-223.
67. Lithium Batteries: New Materials, Developments and Perspectives, edited by C. Julien (Elsevier, 1994).
68. D. D. Yao, J. Z. Ou, K. Latham, S. Zhuiykov, A. P. O'Mullane, and K. Kalantar-zadeh; "Electrodeposited α- and β-phase MoO_3 Films and Investigation of Their Gasochromic Properties" *Crystal Growth and Design*, **2012**, 12(4), 1865-1870.
69. R. Shimizu, K. Yamamoto, T. Suzuki, T. Ohsawa, S. Shiraki, and T. Hitosugi; "Low-Temperature Deposition of Meta Stable β-MoO_3 (011) Epitaxial Thin Film Using Step and Terrace Substrates" *Thin Solid Films*, ***2015****, 595,* 153-156.

70. K. J. Lethy, D. Beena, V. P. M. Pillai, and V. Ganesan; "Bandgap Renormaliztion in Titania Modified Nanostructured Tungsten Oxied Thin Films Prepared by Pulsed Laser Deposition Technique for Solar Cell Applications" *Journal of Applied Physics*, **2008**, 104, 033515.
71. M. Kovendhan, D. P. Joseph, E. S. Kumar, A. Sendilkumar, P. Manimuthu, S. Sambasivam, C. Venkateswaran, and R. Mohan; Structural Transition and Blue Emission in Textured and Highly Transparent Spray Deposited Li Doped WO_3 Thin Films" *Applied Surface Science,* **2011**, 257(18), 8127-8133.
72. P. Skemer and S.-I. Karato; "Effects of Solute Segregation on the Grain-Growth Kinetics of Orthoproxene with Implications for the Deformation of the Upper Mantle" *Physics of the Earth and Planetary Interiors,* **2007**, 164(3), 186-196.
73. H. Reiss; "Rotation and Translation of Island in the Growth of Heteroepitxial Films" *Journal of Applied Physics,* **1968**, 39, 5045.
74. K. Nordlund and R. S. Averback; "Inverse Kirkendall Mixing in Collision Cascades" *Physics Review B,* **1999**, 59, 20.
75. T. Polcar and A. Cavaleiro; "Structure, Mechanical Properties and Tribology of W-N and W-O Coatings" *International Journal of Refractory Metals and Hard Metals*, **2010**, 28(1), 15-22.
76. R.S. Vemuri, G. Carbjal-Franco, D.A. Ferrer, M.H. Engelhard, and C.V. Ramana; "Physical Properties and Surface/Interface Analysis of Nanocrystalline WO_3 Films Grown Under Varialbe Oxygen Gas Flow Rates" *Applied Surface Science*, **2012**, 259, 172-177.
77. N.E. Stankova, P.A. Atanasov, T.J. Stanimirova, A. Og. Dikovska, R.W. Eason; "Thin (001) Tungsten Trioxide Films Grown by Laser Deposition" *Applied Surface Science,* **2005**, 247 (1), 401-405.
78. R.S. Vemuri, M.H. Engelhard, and C.V. Ramana; "Correlation Between Surface Chemistry, Density, and Band Gap in Nanocrystalline WO_3 Thin Films" *Applied Materials and Interfaces,* **2012**, 4(3), 1371-1377.
79. C.V. Ramana, R.S. Vemuri, I. Fernandez, A.L. Campbell; "Size-Effect on The Opitcal Properties of Zirconium Oxide Thin Films" *Applied Physics Letters,* **2009**, 95, 231905.

Curriculum Vita

Gabriel A. Lopez was born in El Paso, TX on October 21st, 1991 where he was raised with three sisters. Gabriel attended El Paso Community College to complete the required core classes for a Bachelor's degree in mechanical engineering. He transferred and obtained a B.S. in mechanical engineering at The University of Texas El Paso (UTEP) where he was awarded for his astounding performance. As an undergraduate, he worked within Dr. Ramana's research group under the PREM program which led him to stay at UTEP for his Master's degree. Gabriel is currently waiting for graduation in December of 2017 for an M.S. in mechanical engineering.

Permanent address: 11124 Montana Ave. Sp.219
El Paso, TX, 79936

This thesis was typed by Gabriel A. Lopez